

SAND81-1025
Unlimited Release
UC-62d

Use of Sandia's Central Receiver Test Facility as a High-Intensity Heat Source for Testing Missile Nose-Cone (Radome) Radar Systems

Donald R. Porter

Prepared by Sandia National Laboratories, Albuquerque, New Mexico 87185
and Livermore, California 94550 for the United States Department of Energy
under Contract DE-AC04-76DP00789

Printed September 1981

***When printing a copy of any digitized SAND
Report, you are required to update the
markings to current standards.***



Sandia National Laboratories

Issued by Sandia National Laboratories, operated for the United States Department of Energy by Sandia Corporation.

NOTICE: This report was prepared as an account of work sponsored by an agency of the United States Government. Neither the United States Government nor any agency thereof, nor any of their employees, nor any of their contractors, subcontractors, or their employees, makes any warranty, express or implied, or assumes any legal liability or responsibility for the accuracy, completeness, or usefulness of any information, apparatus, product, or process disclosed, or represents that its use would not infringe privately owned rights. Reference herein to any specific commercial product, process, or service by trade name, trademark, manufacturer, or otherwise, does not necessarily constitute or imply its endorsement, recommendation, or favoring by the United States Government, any agency thereof or any of their contractors or subcontractors. The views and opinions expressed herein do not necessarily state or reflect those of the United States Government, any agency thereof or any of their contractors or subcontractors.

Printed in the United States of America
Available from
National Technical Information Service
U. S. Department of Commerce
5285 Port Royal Road
Springfield, VA 22161

NTIS price codes
Printed copy: \$ 6.00
Microfiche copy: A01

Use of Sandia's Central Receiver Test Facility as a High-Intensity Heat Source for Testing Missile Nose-Cone (Radome) Radar Systems

Donald R. Porter
Central Receiver Test Facility Division 4713
Sandia National Laboratories
Albuquerque, NM 87185

Abstract

This report describes a series of tests at Sandia's Central Receiver Test Facility in support of the US Navy's SM-2 Blk 2 Radome Improvement Program. The CRTF was the source of high-intensity solar radiation for testing onboard radar-tracking systems under heating conditions intended to simulate those that occur in supersonic flight. Also discussed are the hardware used and the software developed at the CRTF.

Contents

Introduction	7
The Central Receiver Test Facility	7
Test Objectives and Methods.....	9
Test Setup.....	9
Testing Phases	9
Phase I.....	9
Phase II.....	9
Phase III	12
Phase IV	12
Phase V.....	12
Data Processing.....	13
Data Acquisition	13
Data Display and Storage.....	13
Experiment Control.....	13
Satellite Processor.....	13
Test File.....	13
DOPER Program	13
Satellite Program SCAN.....	13
Data Central Operation	17
Data Conversions.....	17
Data Storage	17
Data Display	17
Real-Time	17
Numerical	17
Plotting Capabilities	18
Real-Time Plotting.....	18
Posttest Plotting.....	18
Plotting Boresight Error	18
Plotting the Slope of Boresight Error.....	20
Plotting Temperature vs Position	21
Data Smoothing.....	21
Conclusions.....	21
Reference	23

Illustrations

Figure

1 The Central Receiver Test Facility	8
2 Radome and Test Fixture	10
3 Null-Seeker Antenna	11
4 Data-Acquisition Processors	14
5 The HP9611R Data Station	15
6 Tektronix 4014 Terminal	16
7 Real-Time Numeric Display	18
8 Real-Time Plot	19
9 Plot of Time vs Temperature	19
10 Plot of Boresight Error	20
11 Plot of Boresight Error Slope	21
12a Plot of Smoothed Time vs Temperature	22
12b Real-Time Plot	22

Use of Sandia's Central Receiver Test Facility as a High-Intensity Heat Source for Testing Missile Nose-Cone (Radome) Radar Systems

Introduction

The Applied Physics Laboratory at Johns Hopkins University of Laurel, MD is participating with the US Navy in a series of tests for the SM-2 Blk 2 Radome Improvement Program. Carried out in five phases, these tests were designed to demonstrate the reliability of onboard radar-tracking systems subjected to increased heating of the nose cone (radome) during supersonic flight. The test method involved applying heat to the radome assembly in the form of high-intensity, concentrated solar radiation and then measuring the effects on rf receptions of the missile antenna.

Sandia's Central Receiver Test Facility (CRTF) was the high-intensity heat source for testing. Both the hardware used and the software developed at the CRTF in support of radome system testing are discussed in this report.

The Central Receiver Test Facility

Located on a 100-acre tract of land on Kirtland Air Force Base at Albuquerque, NM, the CRTF (Figure 1) consists of a receiver tower, heliostat field, control room, a lifting module, and cabling and mechanical-equipment rooms. The 200-ft concrete receiver tower is surrounded by a paved area containing an array of 222 heliostats. The tower can accommodate several concurrent experiments in the upper sections of the north face of the tower and on the top. The experiment described in this report was located on a cantilevered platform at the top of the tower. A shaft at the center of the tower accepts a 100-ton-capacity, three-story lifting module. The center floor of this module serves as a temperature-controlled computer room. The upper level is a cabling room; the lower story is a mechanical-equipment room.

A 1500-ft tunnel that is both a personnel access

route and a route for control and data cables connects the tower and heliostat field with a computerized control room. Four computer systems share the tasks of controlling heliostat movement, data acquisition and display, and experiment parameters. These minicomputers are connected in a distributed-system network by means of a serial hardwired link to information-handling hardware at various locations in the tower. Computer-controlled hardware can be moved to any test location in the tower; a full array of equipment that can support a wide variety of solar experiments is located in the lifting module.

Each of the 222 heliostats surrounding the tower is made up of 25 separate facets or mirror sections. These facets are connected to an assembly and can be manually positioned relative to each other. This alignment creates a mirror arrangement that makes the 5x5 facet array closely approximate a parabolic reflector. The assembly is, in turn, fastened to a yoke, allowing the array to be moved in both azimuth and elevation directions. The heliostats are controlled through bidirectional serial links from four minicomputers to hardwired logic at the base of each heliostat assembly. This logic operates two dual-speed servo motors that control the azimuth and elevation positions. Positional data obtained from 13-bit absolute digital encoders and status data from the hardwired logic are sent back to the computer over the same bidirectional link that carries commands to the heliostats.

Analog signals from sensors connected to experiments in the tower are converted to digital information and sent to the minicomputers in the control room where the data are stored and displayed. As many as 512 channels of analog data may be sampled every 2 s, and a subset of these channels may be sampled every second. A complete description of the facility and its capabilities is presented in Reference 1.

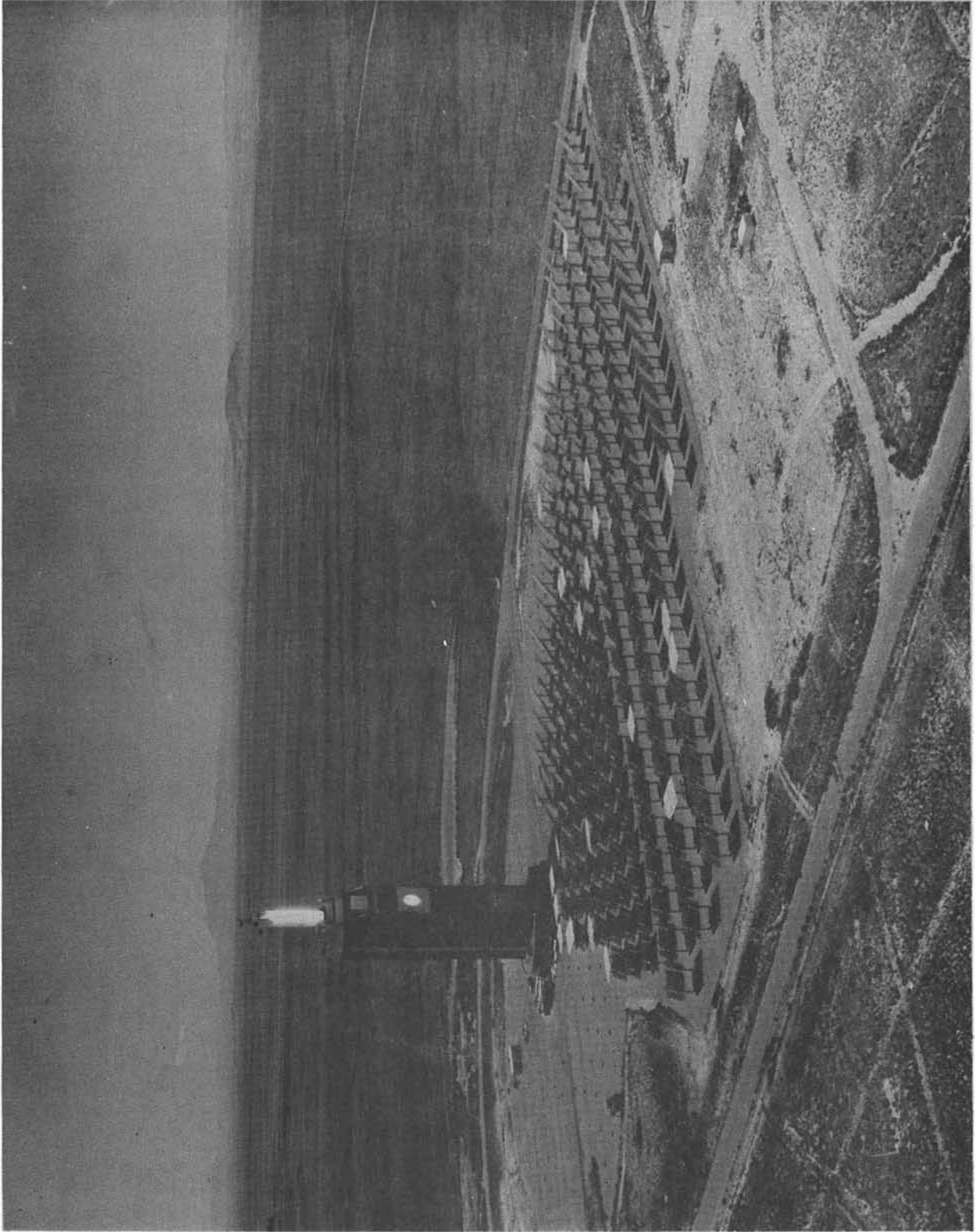


Figure 1. The Central Receiver Test Facility

Test Objectives and Methods

The overall objective of this test program was to verify predicted operation of onboard flight-vehicle tracking systems exposed to supersonic speeds as precisely and completely as possible. Part of this environment is the intense heating of the radome surface that protects the tracking antenna. This heating is expected to influence the ability of the antenna to define a true vector to any target illuminated from a separate radar-transmitting station.

The test method first required establishing a very accurate "boresight," a line-of-sight communication path between a transmitting antenna and a radome-shrouded receiving antenna. Then the radome was heated by solar radiation to simulate heating in the flight environment and moved to simulate a target location off centerline to the missile. The relativity of the radome and airborne antenna forces the receiving antenna to track the signal through a different portion of the radome skin than for a target directly in front of the missile. This change of "look angle" is expected to distort the radar signal, producing an apparent target vector that may be incorrect. The difference between the apparent and true target vectors may be a function of radome look angle and the specific portion of the radome skin in the antenna-to-target path. Further, the degree of look-angle distortion alters significantly as the temperature of the radome increases. What is needed, then, is to fully map the influence of a specific radome on the overall response of the tracking system. This will enable designers not only to design better radomes but also possibly tailor tracking electronics to expect perturbation of antenna signals by the radome surface at given look angles.

Test Setup

Figure 2 shows the radome and its support fixture mounted atop the CRTF tower. At this location the computer-controlled heliostats can be focused on the radome to uniformly heat the entire surface. Data taken from the tower-top hardware were fed to data-acquisition equipment in the tower; these data included radome surface temperatures, flux density levels, and radar antenna look angles. General Dynamics of Pomona, CA supplied and operated the transmitting-antenna assembly that provided the error analysis of the radar antenna signal.

The transmitting antenna was located near the center of the heliostat field to allow the tower-top fixture to point the radome toward the field in both the heating and rf test phases. After the receiving-

antenna and transmitting-antenna assemblies were in place, they were very carefully aligned to give an accurate center-to-center line-of-sight communication path. The transmitting antenna was mounted on a servo-driven device (a null seeker) that allowed four-quadrant movement of the antenna in a plane normal to the antenna-to-antenna boresight (Figure 3). Signals from the four quadrants of the receiving antenna were fed through electronics in the base of the tower and were used by the null-seeker controller.

Responding to the receiving antenna signals, the null-seeker controller moved the transmitting antenna until a signal "null" was reached (all four signals equal). Signals that indicated null-seeker behavior and total rf power received were fed to control hardware in the base of the tower and then back to the control room by means of the tower data-acquisition system.

Testing Phases

Actual testing of radome hardware was in five phases. The amount of data gathered and the method of data storage and display remained essentially the same throughout these five phases, except that Phases I and II required limited-data sets and smaller data files.

Phase I

Phase I was done with the test fixture in place but no radome attached. In its stead was a tree structure with an array of 11 heat-flux calorimeters placed to represent seven different locations on the radome surface. This structure served as a real-time aperture flux gage; in succeeding tests the aperture would be the surface of the radome.

This test, completed in May 1979, demonstrated that the CRTF could provide temperature distributions in missile radomes like those of actual flights.

Phase II

The Phase II tests, which amplified the findings of Phase I, consisted of a missile radome instrumented with 36 thermocouples. Filtered optical pyrometers were also used to measure radome surface temperatures. Specifically, four of these instruments were aimed at various locations on the radome and calibrated against thermocouple readings at these locations. The pyrometers were required for later tests because using thermocouples interferes with radar transmissions.

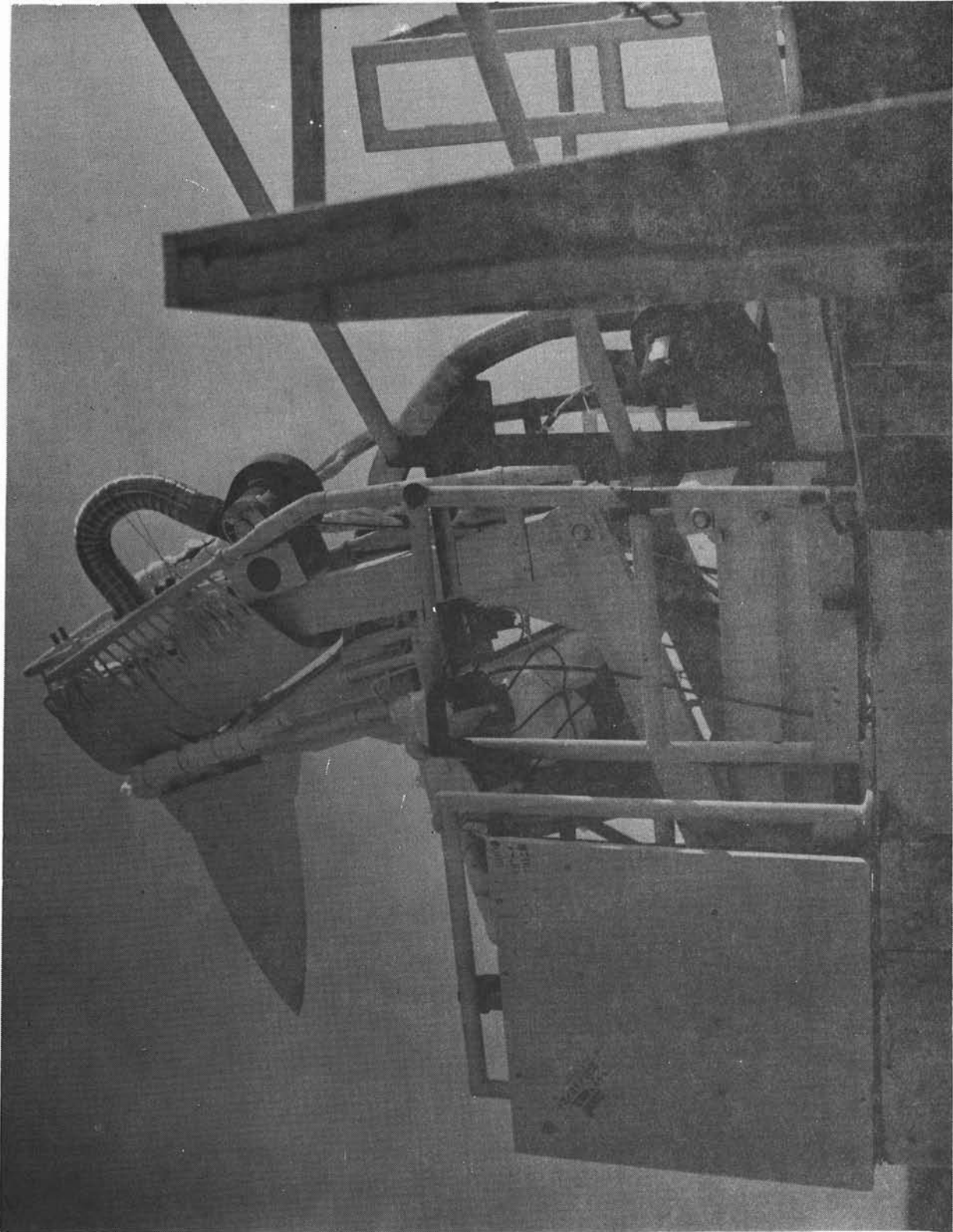


Figure 2. Radome and Test Fixture

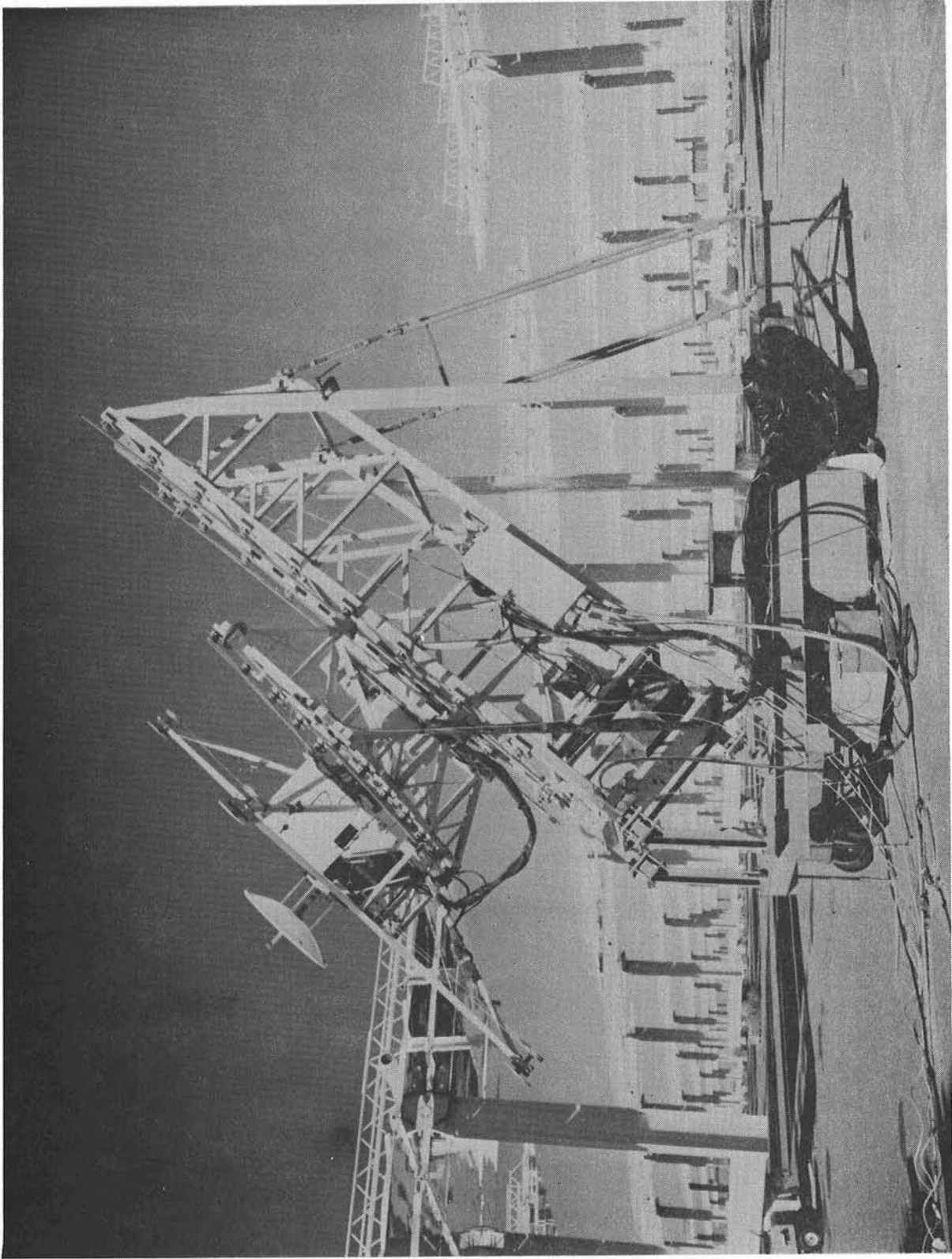


Figure 3. Null-Seeker Antenna

Phase III

During Phase III a few thermocouples were used to measure the temperatures of the radome support hardware, and pyrometers were used to measure the surface temperature of the radome. Calorimeters measured the flux-density levels incident at the base of the radome. Data were also taken from the radome-positioning hardware, and from the null-seeker. All these data were fed back to the computer control room and used to characterize the behavior of the radomes under the test.

Phase III tests began by heating the radome surface. The heliostats were held at standby (an off-target collection point for all heliostat-reflected beams) very near the test hardware to allow rapid application of heat from preselected groups of heliostats arranged to provide several different levels of heating for each test specimen. During heating, surface temperatures of the radome and flux density levels were plotted in real time. Heating continued until a preselected temperature level on the radome surface was achieved; the heliostats were then quickly removed for the boresight error-measurements mode. This phase of the test was designed to define how well the antenna inside the radome could be expected to track a target as the radome was heated.

To simulate an off-line target location, the radar antenna was held stationary on the antenna-to-antenna line of sight, and the radome was moved horizontally from -30° to $+30^\circ$ from direct line of sight with the null-seeking ground antenna. The null seeker was then allowed to track in a plane normal to the line of sight between it and the radar antenna to determine the apparent deflection of the rf signal caused by heating the radome surface. This deflection, recorded as boresight error, was plotted against surface temperature or as a function of radome look angle for various radome temperatures.

The actual rf deflection signal from the null seeker was delivered to the computer in two separate components. One was the in-plane signal deflection, or the apparent error in the same plane as the radome look-angle movement. The other signal was the cross-plane deflection, or the apparent error in the plane perpendicular to the plane of the radome look-angle movement. To completely characterize the effect of the heated radome on the radar tracking signal, these data were recorded for a cold radome; then the hot test was made. For comparison, another run was made after the radome was cooled to ambient temperatures. These three runs or "cuts" completed a test with a particular set of parameters.

Parameters such as rf frequency and the static roll angle of the radome and antenna position were then changed, and a complete sequence of hot and cold cuts was made at the new settings. All data from these runs were then used to provide a map of radome performance. This procedure was repeated for several other radomes.

Phase IV

Phase IV was much like Phase III except that computerized data-plotting routines were required to produce boresight error rate-of-change data for plotting against radome look angles. To make the rate-of-change, or slope, calculations required more accurate and more stable transducer signals than those for Phase III. Low-frequency filters and amplifiers were added in some signal paths to provide the needed signal conditioning.

Phase V

Phase V was a major addition to the test program. Some of the radomes tested were from an advanced SM-3 missile-development program. This new missile is expected to subject the radomes to higher levels of atmospheric heating, and Phase V was designed to simulate these new heating levels. Some changes were made in the instrumentation package and procedures to better define the physical response of the radomes to the increased heat load and heating rates. Six high-temperature resistive strain gages were cemented to the inner surface of a blackened radome. The radome surface was painted black to increase absorptivity, allowing a higher heating rate and higher ultimate temperatures.

To achieve a very fast temperature rise time, a shutter was used. This shutter, a solar-protected panel, was suspended directly in front of the radome. The heliostats were focused on the target as in previous tests, but the radome remained in the shadow of the shutter until all the heliostats were focused. The shutter was then allowed to rotate out of the path of the solar beam and expose the radome.

This was to be a destructive test. The radomes were not expected to survive these temperatures, and they did not. Before they broke, however, valuable information was collected and recorded about stress patterns present in the heated radome. This information will be used for correlation with data from computer models written to predict stress patterns.

Data Processing

Data Acquisition

The equipment purchased from Hewlett-Packard as part of the overall distributed-computer network provides a flexible and effective data-acquisition system (DAS) (Figure 4). The DAS includes a central processor, a dedicated satellite computer, and three remotely operated data-handling units (HP9611R). One HP9611R operates the facility's heat-rejection system (HRS); the second is located in the lifting-module computer room and is used for experiments on or near the module; and the third is a floating system locatable anywhere. Figure 5 shows the HP9611R system in the module computer room.

Each HP9611R remote system has two major parts. The first is an analog-to-digital conversion system (HP2313) with a maximum capability of 512 channels, a maximum sensitivity of ± 5 V, and a range of ± 10 V. The second part of the HP9611R is an HP6940 multiprogrammer that provides input and output of voltages, output-control currents, and switch-closure outputs. This facility uses the voltage and current outputs to control experiment conditions from the control room. The switch-closure output capability is also used extensively for control of remote experiments.

Data Display and Storage

Data obtained by the HP9611R is transferred from the satellite computer to the central processor over a computer-to-computer link. The data computer has several tasks, including storage of the data in raw voltage form, conversion of the data to engineering units, display of data for the experiment operator, storage of selected data in engineering unit form, and posttest data reduction. These functions are described in detail later in this report.

One display requirement is to pass on display parameters to the facility control computer so that color graphics may be used to display both control and experiment information. Both types of information may be displayed for the experimenter and the facility control operator.

Experiment Control

Several computer peripherals are connected to the data processor to display and control experiment parameters. Five data displays can be programmed to accept experimental data; one of these is a Tektronix 4014 terminal that allows full graphics capability

with excellent resolution. A 4631 hard-copy unit provides real-time hard copy of information displayed on the terminal (Figure 6).

Satellite Processor

The data central computer runs a manufacturer-supplied real-time executive system called RTE-3, which allows development of an RTE-C software system that can be sent from data central over the computer-to-computer link to the satellite processor. RTE-C is a true real-time system running in a memory-only environment (it has no disk memory). Once running, more communication can occur between the data central and the satellite processor by means of the computer-to-computer link.

Test File

The HP6911R hardware located in the tower can convert voltages to digital signals from up to 521 separate channels with a range of inputs ± 0 to 10 V, in 5-mV steps. A test file is used to define which channels will be sampled and at what intervals. Also, the test file defines what voltage should be expected on each channel and how much gain should be used to get the best resolution possible. A program that runs in the data central processor allows an operator to design the test file to best suit the experiment. The test file is stored on the disk memory for later access.

DOPER Program

A Data Operation Program (DOPER) is run so that the operator uses the test file to tailor the satellite operating system to the data-acquisition task. DOPER first asks the operator to name a raw-data storage file on the disk memory. The program then accesses the test file and composes a block of information to send over the link to the satellite. This information is used by the satellite processor to command the HP2313 data system.

Satellite Program SCAN

A satellite program, SCAN, is initiated from the data processor and runs at operator-selected intervals. SCAN uses the information taken from the test file to command the HP2313 and begin data conversion on the selected channels. After SCAN receives data from the tower hardware, the XMTR program transfers data across the link to the data processor and then schedules the XMTC program, which receives SCAN data from the link and converts them into a more usable form.

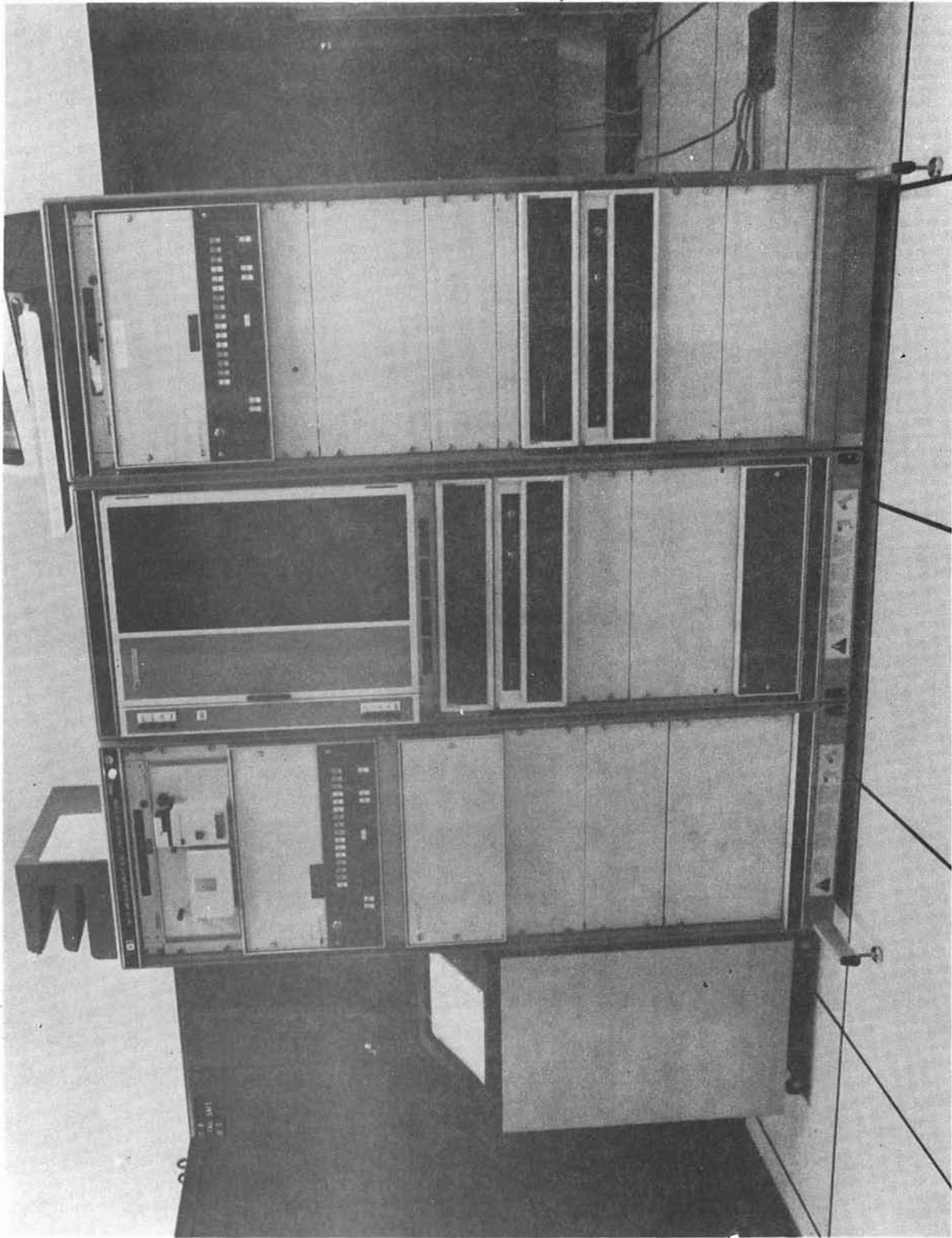


Figure 4. Data-Acquisition Processors

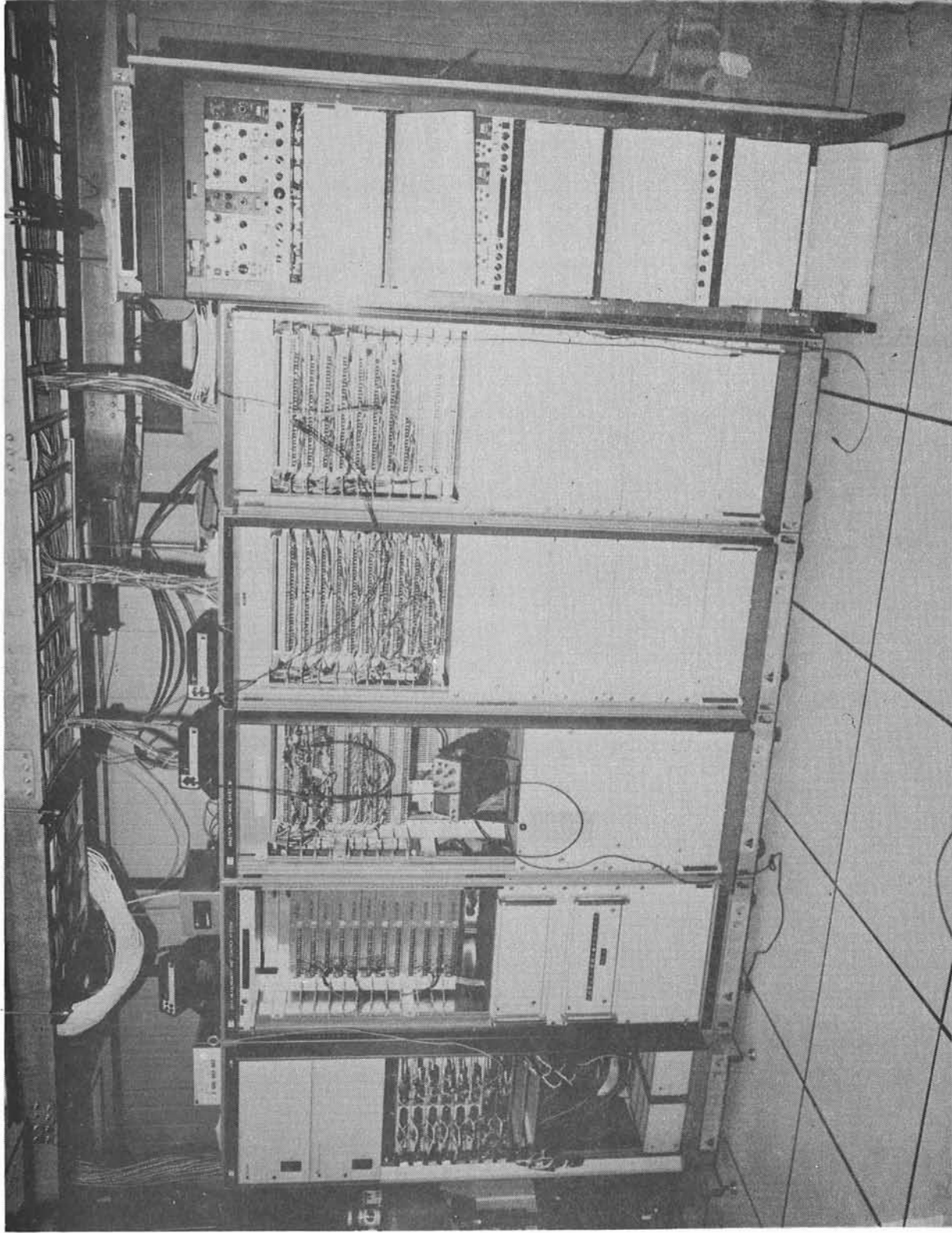


Figure 5. The HP9611R Data Station

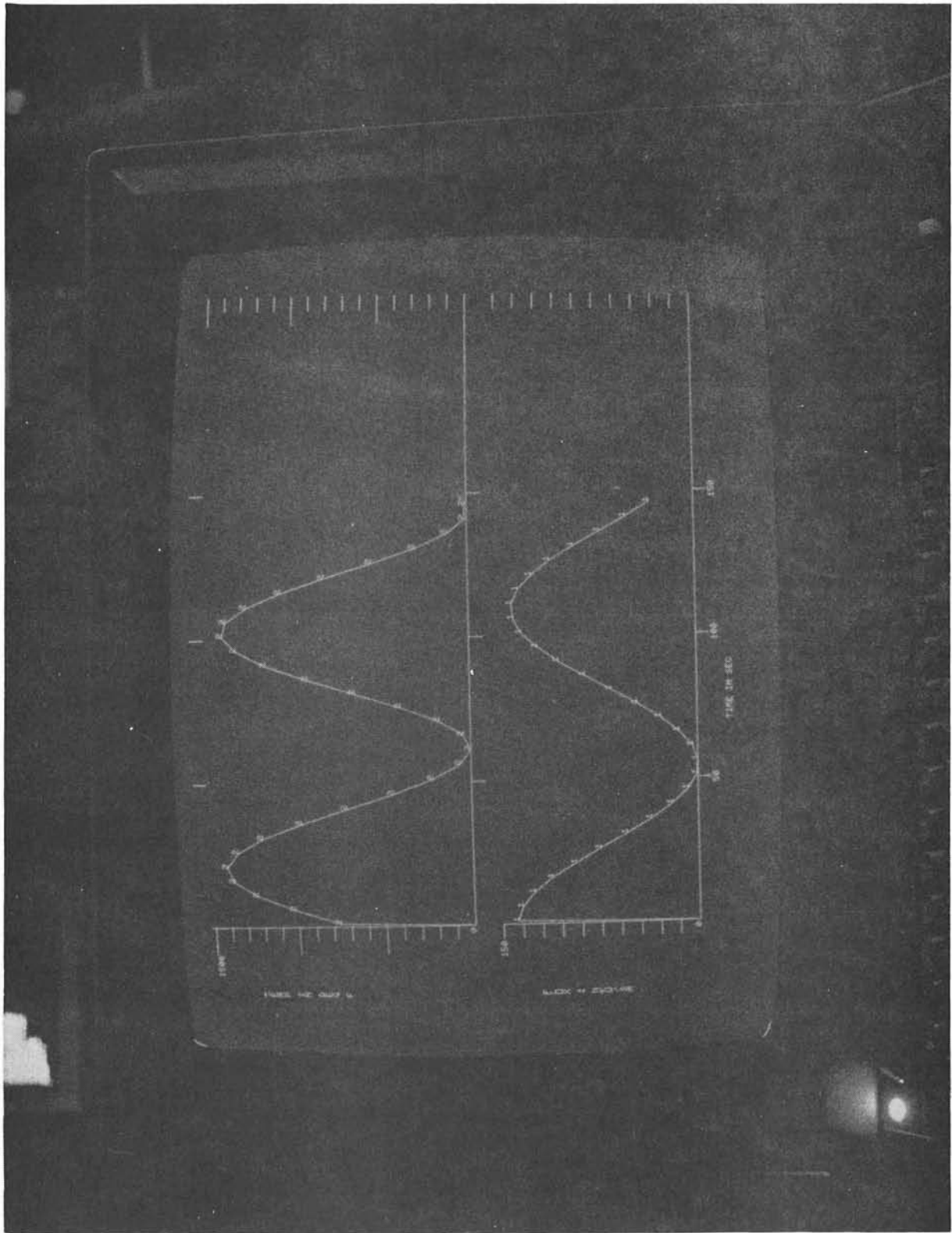


Figure 6. Tektronix 4014 Terminal

When data are to be sent to the HP6940 hardware in the tower for experiment control, the central data processor sends the data over the link and schedules a DN694 program in the satellite. When DN694 runs, it accepts data from the link and sends the command to the hardware in the tower.

Data Central Operation

XMITC accepts data from the satellite and places it in short-term storage. This raw-data file, located in disk memory, accepts data from one day's testing. The data must then be transferred to long-term storage on magnetic tape at the end of each day's testing. Data are stored just as received from the tower hardware: one 16-bit word for each channel sample, with 12 bits of voltage plus a 3-bit gain figure. One bit is included to indicate if the channel was forced to automatic-range. Automatic ranging occurs if the HP2313 hardware detects a signal that, when multiplied by the test file's gain set, is $> \pm 10$ V. The gain is then changed until the signal no longer overranges the hardware. This gain is then attached to the data word and the automatic-range bit is set.

Two other sets of parameters are included along with the data block from the satellite. One is a five-word data set defining the time at which the data scan was initiated. The other is an eight-word set defining which of eight possible frequency blocks was sampled in any given data scan. The eight frequency blocks are defined by the test file and used to determine which groups of channels are to be sampled on any particular data scan. If this frequency-block information and the data from the test file are used, a data-reduction program can find out which channels were sampled in any one data scan. The XMITC program then places the blocks of raw data into a special area of computer memory ready to be accessed by a data-display software package.

Data Conversions

For this series of tests a maximum of 45 channels of information were sampled once a second. At the CRTF the normal data storage sequence is to store the raw voltage data on a disk file, then convert a subset of that data to engineering units (temperature, flux, position, etc) for display in real time.

In this case the relatively small volume of data allowed all the data to be converted to engineering units in real time and stored on a disk file in that form; the raw data were not saved. Thermocouple signals were converted to temperature by using a

segmented polynomial equation. Other signals were treated as linear responses, and voltage signals were converted to engineering units by using manufacturer-supplied calibration figures. Angular displacement signals were calibrated online by physically moving the hardware to several known positions and noting the voltage presented to the instrumentation system. This method produced a linear calibration between several defined operating points.

Data Storage

A normal data-handling sequence at the CRTF would be to store raw data on disks as the test is run continuously through the day, and to discard data converted online for display. After the daily test is over, the raw data are retrieved from the disk file, converted to engineering units, and then stored on magnetic tape—a process that takes about 1 h for every 3 h of data taken.

In the case of the radome experiment, data were taken throughout the day from several tests of short duration, converted to engineering units in real time, and then stored in disk files unique to particular runs. These data included information acquired every second and tagged with the time taken. Data from a particular test run may be picked up from the disk file and plotted any time after the run is completed. Specific data to be plotted may be bounded by time limits or by an event signal included in the data that marks significant events in the run. Data in these disk files may be moved to magnetic tape for archiving or for transportation to another facility for further analysis.

Data Display

Real Time

During a test run the sampled data are being converted from voltage form to temperatures, flux density levels, and angular displacement. While all these data are being stored on disk memory, a subset of data can be displayed to establish operating characteristics of the hardware.

Numerical

Numerical display in real time of each datum is provided on a CRT screen and updated about every 2 s. This display is provided mainly as a diagnostic, because the numbers change too quickly for a qualitative analysis of several channels in real time. Figure 7 shows a real-time numerical display.

```

DATA TIME= IHR=10   MIN=49   SEC=53   JP== 3

TEMPS=  45    43    44    44    44    43    44
PYROS= 401   481   400   400   101   1541  1352
NSX NULL SEEKER      X      MRAD=  1.1780
NSY NULL SEEKER      Y      MRAD=  -.0645
RAXR RADOME ROTATION      DEG=  .3300
RAZR RADOME AZIMUTH      DEG= -18.3964
SMAP ANTENNA ROTATION      DEG=  -.1000

AIR TEMP=  43 F      INSOLATION= .0024      ISOLATION=1.1976
01= 401.2930 11= .1900 21= 52.5000 31=9999.9004 41= .0000
02= 480.5325 12= .0050 22= 44.9082 32=9999.9004 42=  1.1780
03= 400.4650 13= .0050 23= 43.0959 33=9999.9004 43=  -.0645
04= 400.0000 14= -.0100 24= 44.0023 34= .0024 44=  -.9687
05= 100.8250 15= .0050 25= 44.0023 35=  -.9687 45=  -.9687
06=1540.6851 16= .0100 26= 44.0023 36=  -.9687 46=  .3300
07=1351.5750 17= .0000 27= 43.0959 37=  -.9687 47= -18.3964
08= .6800 18=  -.2400 28= 44.0023 38=  .0325 48=  -.1000
09= .4550 19=  -.0700 29=9999.9004 39=  .0013 49=  -.9687
10= .3100 20= 43.7000 30=9999.9004 40=  .0000 50=  -.9687

```

Figure 7. Real-Time Numeric Display

Plotting Capabilities

Real-Time Plotting

A Tektronix 4014 terminal is used to provide a subset of incoming data as a function of time. This plotting allows observation of the rate of change and current values of the data being plotted. Figure 8 shows a completed real-time plot. Completed plots can be transferred to a Tektronix 4612 electrostatic hard-copy unit. The hard-copy medium is black-on-white paper that is silver-oxide-coated and heat-treated. The real-time plot package may split the screen into top and bottom halves. The top half is scaled to display radome surface temperatures, while the bottom half is scaled to accept data representing flux densities incident on the radome surface. Both halves are plotted against time on identical scales. The divided screen was not needed, for the Phase IV tests, and the entire display area was used to display surface temperatures. Figure 6 shows how the divided screen looked with checkout data. Figure 8 shows a Phase IV real-time data plot.

Posttest Plotting

After each test run, the operator saves the data from that run in a reserved portion of the disk memory. That data may then be accessed to provide a variety of types of data display.

Two modes of selecting a data window are available. The operator may select a start-and-stop time associated with the stored data; the plot package then uses only the data between those two times to generate an actual plot. The other method is to select two excursions of an event signal included in the data. This signal is generated and recorded as a function of physical events occurring during the test run. The plot package looks for these two levels of the event signal and generates the plot by using only data between those two levels.

Data from any of the channels of information may be plotted against time over the selected window. This may be a single channel or multiple channels in the same window. Figure 9 shows a plot against time.

If the time in the data file is not known, the operator may request the first and last data times in any data storage file. This information may be used to set the time window of the plot.

Plotting Boresight Error

For this plot, the signal representing the apparent error in the alignment of the antennas (boresight error) is plotted against the angular displacement (or look angle) of the radome. Look angle is plotted on the horizontal (X) axis, and boresight error on the

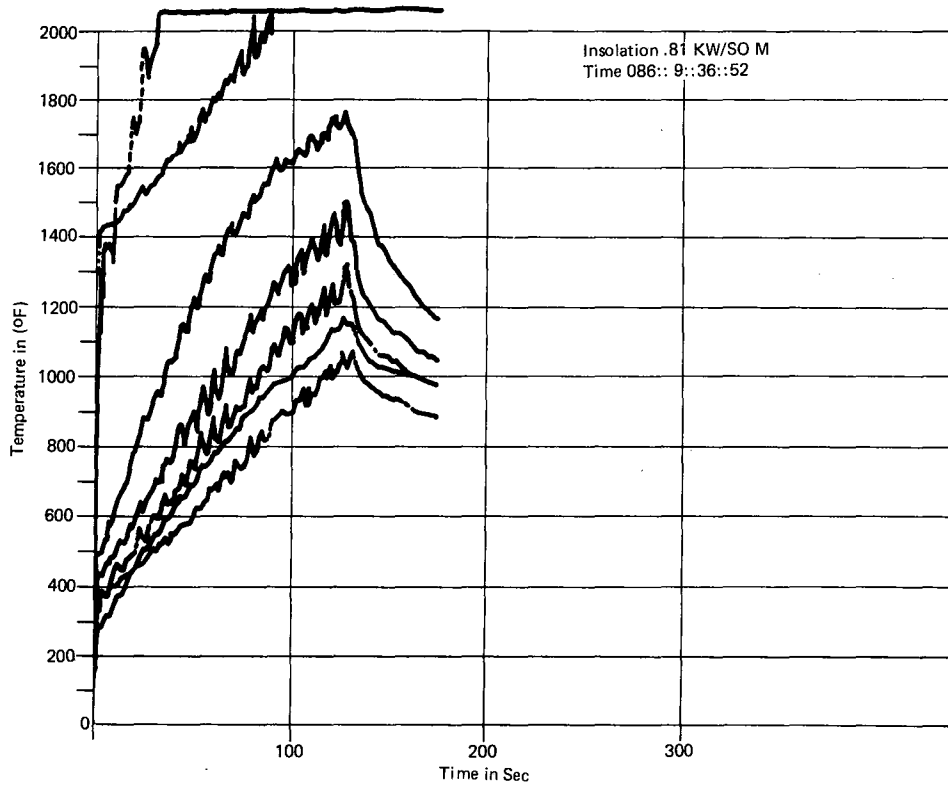


Figure 8. Real-Time Plot

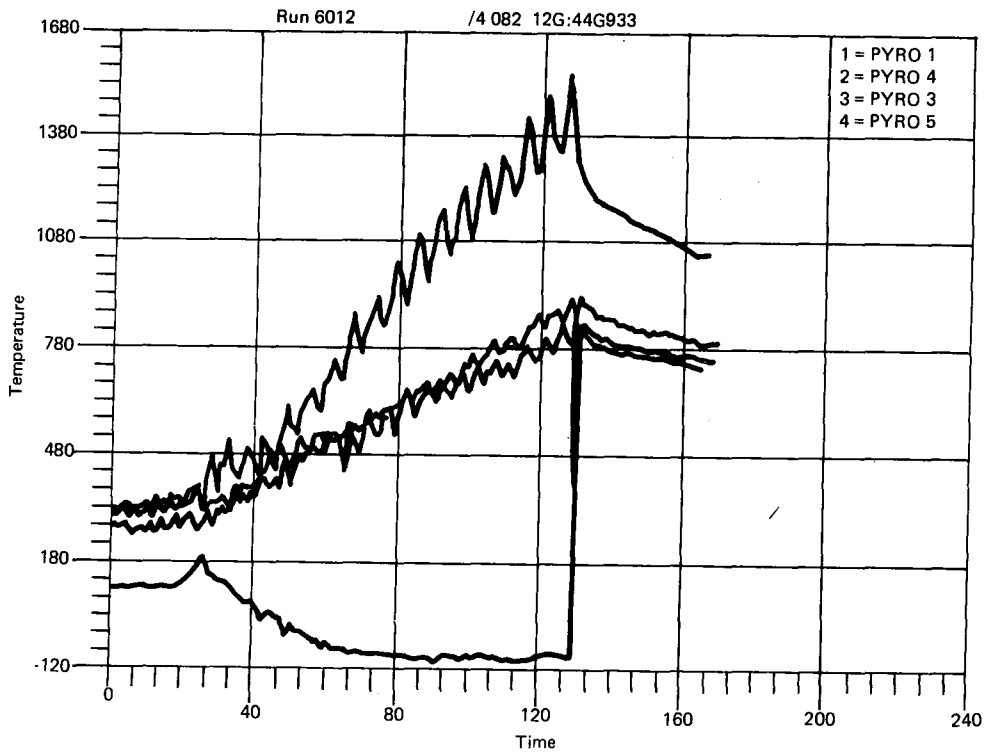


Figure 9. Plot of Time vs Temperature

vertical (Y) axis. The ordinate (0,0) point is in the center of the graph and allows positive and negative values for both look-angle and boresight error. Figure 10 shows a plot of boresight error.

Plotting the Slope of Boresight Error

The plot of boresight error slope begins with the same data used in the boresight error plot. This option is used to establish the change rate of boresight error. One requirement of this plot is to display data in a format directly comparable to that for plots made by General Dynamics in their laboratory tests on the same radome at Pomona, CA.

The horizontal axis (or look angle) ranged from -30° to $+30^\circ$ at a resolution of $10^\circ/\text{in}$. The vertical axis (or error slope) represented a range of -0.04° to $+0.04^\circ/\text{in}$, with a resolution of $0.01^\circ/\text{in}$. Figure 11 plots boresight error slope.

Another requirement for plotting along the horizontal axis was that the data occur at even, 1° increments. (General Dynamics took laboratory data at even-degree increments.) At the CRTF the data were taken at intervals of ~ 1 s, which produced look-angle data of more random values. To match the General Dynamics data, the recorded data were used to produce a close approximation of what the data

would have been at even-angle displacements. Figure 11 graphically shows the process: beginning at the maximum negative excursion of look angle, an even value for look angle is chosen. The sampled data for that channel are then examined and the closest look-angle readings (one on either side of the selected value) are found. The two respective values for boresight error are used to interpolate a third value for boresight error at the chosen value for look angle. The look angle is incremented by one and the process repeated until values exist for all even values of look angle from -20 to $+30$ s.

Boresight error slope was calculated by using the interpolated values for look angle. Using a data window of variable length set by an operator input and starting at the negative excursion of look angle, we summed the errors and divided them by the length of the window in degrees. This first derivative (or slope) of boresight error is then assigned to a look angle in the center of the window. The data window is shifted 1° , and slope is again calculated over the width of the window. This process was continued until boresight error slope was calculated over the entire excursion of the look angle.

These data were then plotted and copied.

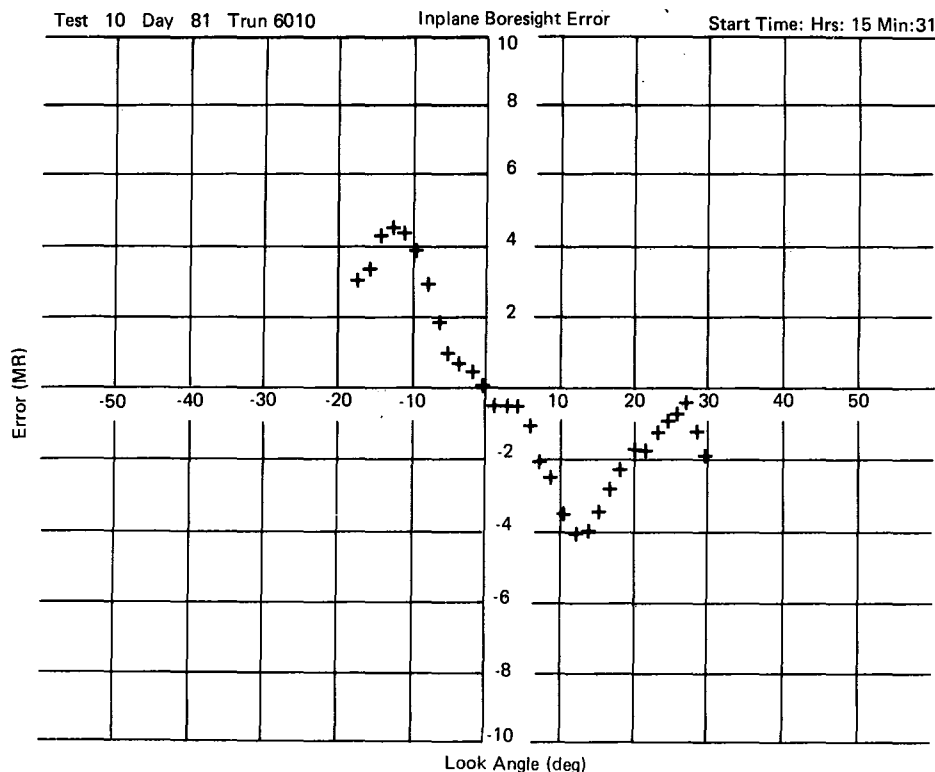


Figure 10. Plot of Boresight Error

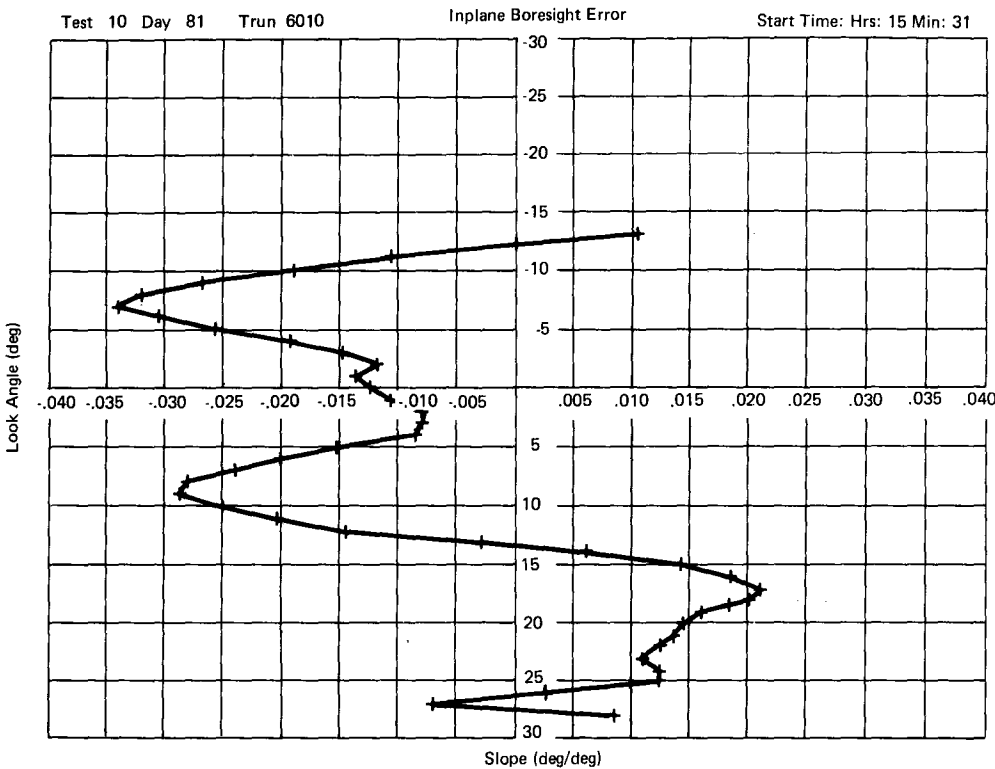


Figure 11. Plot of Boresight Error Slope

Plotting Temperature vs Position

Data for temperature on the surface of the radome are plotted against the respective position on the radome. For this plot the vertical axis is temperature and the horizontal axis is radome surface position. The data are selected at one specific time in the test history, and all temperatures are taken from one data scan at that time.

Data Smoothing

Data from some of the sensors, especially the pyrometers, include a lot of high-frequency noise on a low-frequency data pattern. The smoothing algorithm exposes the true nature of the measured phenomenon. This smoothing algorithm sums a group of data points in a time window and divides the sum by the number of readings to give a simple average. The simple average is assigned to a time near the center of the window; the window is then moved one data sample and the process repeated. The result is an average history over the length of the run. The data

are then plotted and copied. Figures 12a and Figure 12b show the result of data smoothing. Figure 12a is a real-time plot; Figure 12b is a time-history plot with smoothing.

Conclusions

The time limits imposed on the Radome Test Program by CRTF did not allow completion of every combination of test parameters in the test matrix. However, the tests that were run represented all the most important items in the test plan, and most were judged quite successful.

The CRTF proved an excellent source of electrical-ly clean, high-intensity heat, and the data taken showed good agreement with data taken at other test sites.

Information from this test sequence will prove valuable for radome testing in particular and for the US Navy's advanced-missile development programs in general.

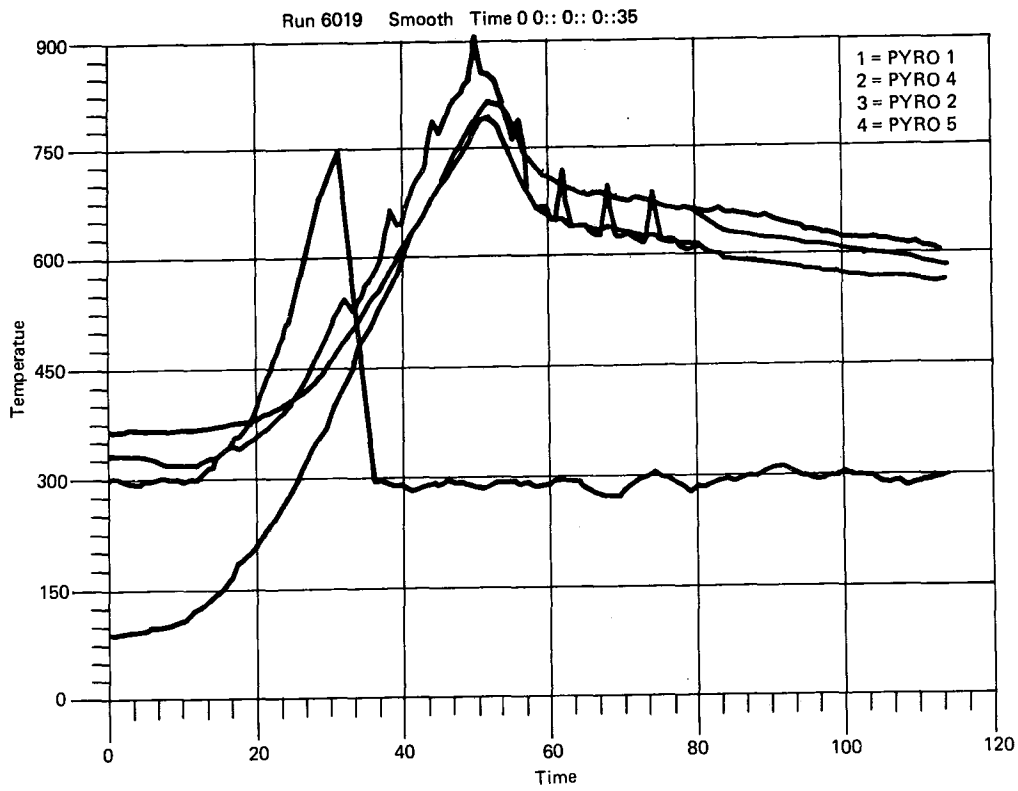


Figure 12a Plot of Smoothed Time vs Temperature

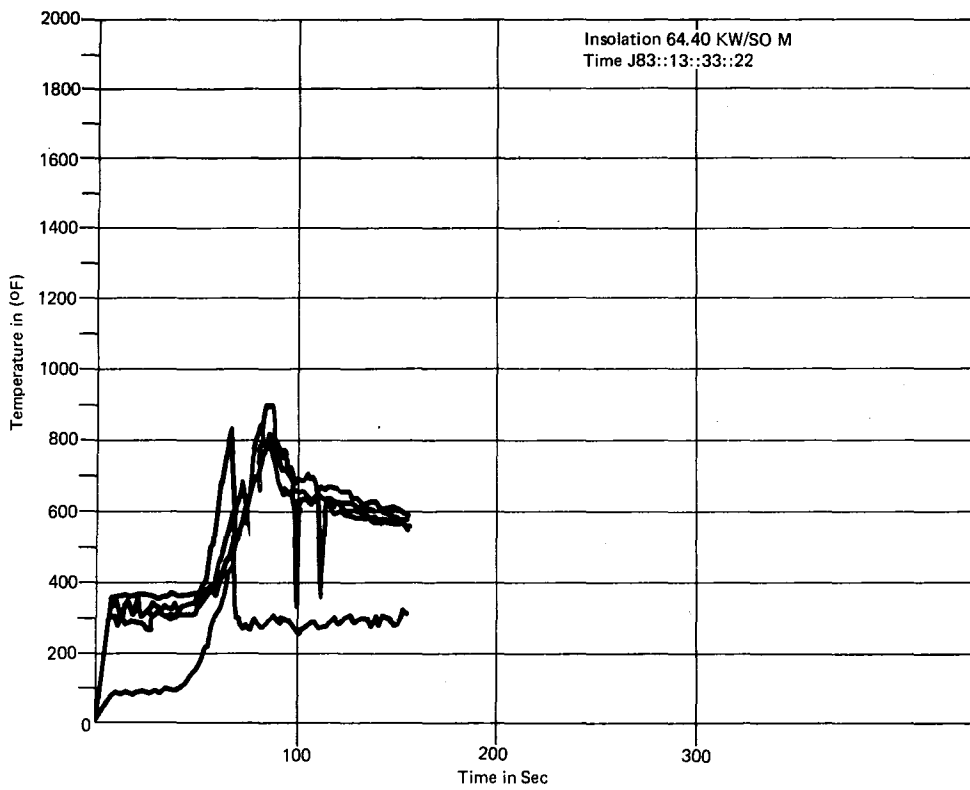


Figure 12b Real-Time Plot

Reference

¹John T. Holmes, et al, *CRTF Experiment Manual*, SAND77-1173
(Albuquerque: Sandia Laboratories, October 1979).

DISTRIBUTION:

TIC-4500-R69 UC-62d (273)

US Department of Energy, STPS (7)
6th and E. Street
Washington, DC 20545
Attn: G. W. Braun (3)
W. Auer
J. E. Runnels
M. U. Gutstein
L. Melamed

US Department of Energy (3)
San Francisco Operations Office
1333 Broadway
Oakland, CA 94612
Attn: R. W. Hughey
S. D. Elliott (2)

US Department of Energy (2)
Albuquerque Operations Office OPEP/SED
Kirtland AFB
Albuquerque, NM 87115
Attn: J. Weisiger
G. Pappas

US Department of Energy, STMPO
5301 Bolsa Ave MS 14-1
Huntington Beach, CA 92647
Attn: R. N. Schweinberg

Solar Energy Research Institute (5)
1536 Cole Blvd.
Golden, CO 80401
Attn: M. D. Cotton
B. P. Gupta
J. P. Thornton
K. J. Touryan
A. Rabl

Aerospace Corp., Suite 4040
955 L'Enfant Plaza, S. W.
Washington, DC 20024
Attn: J. F. Woolley

Solar Thermal Test Facilities/
Users Association (2)
First National Bank, East
Suite 1204
Albuquerque, NM 87108
Attn: F. B. Smith

Georgia Institute of Technology
SEMTE/EES
Atlanta, GA 30332
Attn: T. Brown

White Sands Missile Range
STEWS-TE-AN
White Sands, NM 88002
Attn: R. Hays

University of Houston (2)
Solar Energy Laboratory
Houston, TX 77004
Attn: A. F. Hildebrant

Centre National de la Recherche Scientifique (2)
Odeillo, B. P. 5.
66120 Font-Romeu
France
Attn: C. Royere
D. Gauthier

Applied Physics Laboratory (25)
Johns Hopkins University
Johns Hopkins Road
Laurel, MD 20810
Attn: T. J. Hoyer
L. B. Weckesser
R. K. Frazer
J. R. Kime

1 G. Dacey
4000 A. Narath
4700 J. H. Scott
4710 G. E. Brandvold
4713 J. V. Otts
4713 J. T. Holmes
4713 D. L. King
4713 S. Dunkin
4713 P. Brooks
4713 P. Flora
4713 B. O. Ellis
4713 A. Vance
4713 C. Maxwell
4713 D. B. Davis
4713 R. M. Edgar
4713 R. D. Aden
4713 W. H. McAtee
4713 D. L. Risvold
4713 C. W. Matthews
4713 D. E. Arvizu
4713 M. C. Stoddard
4713 J. M. Stomp
4713 D. R. Porter (10)
4714 R. P. Stromberg
4716 J. F. Banas
4717 J. A. Leonard
4721 W. P. Schimmel (2)
4723 D. G. Schueler (Actg)

DISTRIBUTION (cont):

4756 H. M. Dood
8400 L. Gutierrez
8450 L. Gutierrez (Actg)
8451 C. S. Selvage (Actg) (4)
8452 A. C. Skinroad

8453 W. G. Wilson
8214 M. A. Pound
3141 L. J. Erickson (5)
3151 W. L. Garner (3)
For: DOE/TIC (Unlimited Release)